Springer

KSME

Journal of Mechanical Science and Technology 26 (7) (2012) 2213~2225
www.springerlink.com/content/1738-494x
DOI 10.1007/s12206-012-0303-0

Thermodynamic model for prediction of performance and emission characteristics of SI engine fuelled by gasoline and natural gas with experimental verification †

Dashti Mehrnoosh[1,*], Hamidi Ali Asghar[2] and Mozafari Ali Asghar[3]

[1]*Graduate School of the Environment and Energy, Science and Research Branch, Islamic Azad University, Tehran, Iran*
[2]*Department of Chemical Engineering, University of Tehran, Iran*
[3]*Department of Mechanical Engineering, Sharif University of Technology, Iran*

(Manuscript Received June 17, 2011; Revised December 14, 2011; Accepted February 3, 2012)

Abstract

In this study, a thermodynamic cycle simulation of a conventional four-stroke SI engine has been carried out to predict the engine performance and emissions. The first law of thermodynamics has been applied to determine in-cylinder temperature and pressure as a function of crank angle. The Newton-Raphson method was used for the numerical solution of the equations. The non-differential form of equations resulted in the simplicity and ease of the solution to predict the engine performance. Two-zone model for the combustion process simulation has been used and the mass burning rate was predicted by simulating spherical propagation of the flame front. Also, temperature dependence of specific heat capacity has been considered. The performance characteristics including power, indicated specific fuel consumption, and emissions concentration of SI engine using gasoline and CNG fuels have been determined by the model. The results of the present work have been evaluated using corresponding available experimental data of an existing SI engine running on both gasoline and CNG. It has been found that the simulated results show reasonable agreement with the experimental data. Finally, parametric studies have been carried out to evaluate the effects of equivalence ratio, compression ratio and spark timing on the engine performance characteristics in order to show the capability of the model to predict of engine operation.

Keywords: CNG; Engine performance; Gasoline; SI engine; Thermodynamic modeling

1. Introduction

Decreasing world energy resources and the problems caused by increased pollutant emissions have resulted in a great deal of efforts on the development of alternatives for fossil fuels in internal combustion engines [1, 2]. A large number of studies have been on the development of internal combustion engines to address technological, environmental and economical concerns [3]. Recently Taylor [4] reviewed improvements which have been implemented on internal combustion engines. One of the promising alternative fuels to gasoline in the internal combustion engine is natural gas [5-9]. There are two important advantages in the use of compressed natural gas (CNG) as an alternative fuel, namely, higher thermal efficiency due to the higher octane number and lower exhaust emissions as a result of the lower carbon to hydrogen ratio of the fuel [10]. Also, the abundance and availability of natural gas reserves in comparison to the petroleum resources is another feature of using CNG as alternative fuel in the passenger vehicles engines as well as stationary ones. Many studies and experimental works have been carried out on CNG fuelled engines which were reviewed by Cho and He [10].

Ristovski et al. [11] presented a comparison between the emissions for a modified six cylinders Ford SI engine before and after converting from gasoline to CNG mode. The results showed lower concentrations from 561 to 390 gr/km for CO_2 and 219.7 to 0.891 gr/km for CO emissions. However, the NO_x emission increased from 5.68 to 8.34 gr/km. They claimed that their results were in the range of emissions quoted in the literature.

Aslam et al. [12] carried out an experimental study on retrofitted gasoline SI engine fuelled with CNG. The authors observed a 16% reduction of BMEP due to lower flame speed and a 17-18% reduction of BSFC due to higher heating value of CNG when compared to gasoline. The results showed 20%, 80% and 50% lower levels of CO_2, CO and UHC emissions, respectively. However NO_x production increased by 33%. The lower CO_2 and CO emission is attributed to the lower carbon to hydrogen ratio of CNG and the higher NO_x emission is due to combustion of leaner mixture and higher combustion temperature of CNG compared with gasoline.

*Corresponding author. Tel.: +982144865320, Fax.: +982144860002
E-mail address: mdashti@srbiau.ac.ir
† Recommended by Associate Editor Kyoung Dong Min
© KSME & Springer 2012

Shamekhi & Khatibzadeh [13] carried out a comprehensive experimental study on a bi-fuel four cylinders SI engine in full and part load conditions over a wide range of engine speeds. Engine performance and emissions were also measured for both gasoline and CNG fuels. The authors reported that torque, power and BMEP decreased by approximately 10.8 to 14% due to lower volumetric efficiency of CNG operation. The average of BSFC reduction was between 15 to 24% as a result of higher heating value and leaner combustion of the CNG fuel. Compared to gasoline operation, CO_2 and CO reduction of between 0-11% and 58-89%, respectively, were observed. The leaner combustion of CNG resulted in lower CO production, whereas the higher hydrogen to carbon ratio of CNG causes CO_2 reduction. The results showed considerable reduction in UHC emissions, 37-58% and an increase of NO_x emissions. These can be attributed to higher combustion temperature and leaner mixture when using CNG. They also found that at full load, the MBT spark timing for CNG was between 7 and 13 degrees crank angle more advanced than that of gasoline which results in the higher combustion temperature when using CNG.

For prediction of the internal combustion engine behavior and determination of the trends for different fuels over a wide range of design and operating variables, thermodynamic modeling is a very useful tool. Various models describe the thermodynamic [14], fluid flow, heat transfer and burning rate [15-17], combustion, kinetics and its effective parameters [18-24]. Also, power cycle modeling has been developed in numerous studies to predict engine operating characteristics. Recently Sheppard and Verhest [25] have reviewed the multi-zone thermodynamic models for SI engines.

Benson et al. [26] have reported a comprehensive procedure for simulating the power cycle of a single cylinder four stroke spark ignition engine with the consideration of compression, combustion, expansion and gas exchange processes. They investigated a four steps simulation model for combustion process and used two-zone model to describe the flame front propagation in the cylinder considering ignition delay period. The equilibrium constant method has been applied to determine chemical concentration of eight species. In-cylinder pressure and burned and unburned temperature were reported. In this work, the effect of flame factor on the flame speed and concentration of nitric oxide has been investigated. Also, they studied the effect of air-fuel ratio on cylinder temperature and nitric oxide concentration and compared the results with corresponding experimental data.

A first and second law thermodynamic analysis of a real spark ignition engine cycle has been developed by Rakopoulos [27]. The two-zone model for the combustion process, accurate simulation of the spherical flame front propagation and calculation of eight chemical species concentration were taken into account to predict in-cylinder pressure, nitric oxide emissions and cylinder charge availability of the engine as a function of equivalence ratio. A numerical solution was used to solve the system of nonlinear equations. Validation of the thermodynamic analysis of cycle was carried out by comparing the theoretical findings with the relevant experimental results obtained from a flexible, variable compression ratio, Ricardo E-6 SI engine.

Alla [28] proposed an arbitrary heat release formula to simulate the heat transfer and predict performance of a four stroke SI engine. The effects of equivalence ratio, spark timing, combustion duration, and compression ratio on the engine performance characteristics including BMEP, BSFC and brake thermal efficiency were investigated. The results from the model for cylinder pressure diagram and the predicted performance characteristics of the engine showed good agreement with the measured data.

An analytical model has been developed by Eriksson and Andersson [29] for describing the variation of the cylinder pressure in a SI engine. This model is based on parameterization of ideal Otto cycle and a set of tuning parameters with physical meanings has been used. The results have been validated with experimental data.

Caton [30] has developed a thermodynamic simulation for the SI engine cycle. He studied the maximum temperature of the cylinder with respect to fuel-air ratio, compression ratio and spark timing using three-zone model for the combustion process. The burned gases were divided into burned zone, an adiabatic core and boundary layer and the second law of thermodynamic was considered for simulation. The comparison of the results from the multiple zone simulation with the results from a similar single zone model was carried out and it was shown that the use of a multiple-zone model for engine cycle simulations provides additional insight into the major processes relative to the use of a single zone approach. In another study [31], Caton investigated the effect of compression ratio on nitric oxide emissions of the SI engine. He used the three-zone thermodynamic model for prediction of nitric oxide emissions as a function of compression ratio. The computed results were shown to be compatible with experimental results from the literature.

Finite-time thermodynamic modeling of an air-standard Otto cycle with consideration of variable specific heats of the working fluid and heat transfer loss has been reported by Ge et al. [32]. The authors assumed that the heat loss through the cylinder wall was proportional to average temperature of both the working fluid and the cylinder wall. They investigated the relations between the power and thermal efficiency of the engine as a function of compression ratio. The results showed that the temperature dependence of specific heat and heat loss of working fluid should be considered in the cycle analysis due to their effects on engine power and efficiency. Also, in another work by Abu-Nada et al. [33] the mentioned effect on cylinder pressure and temperature, BMEP and thermal efficiency of engine were confirmed by thermodynamic simulation of air-standard Otto cycle.

A computer simulation of four stroke CNG SI engine has been carried out in Ref. [34]. The authors optimized performance characteristics of the engine by employing cooled ex-

haust gas recirculation at high inlet pressure at stoichiometric condition. They used two-zone combustion model with eight species as products and Wiebe function for calculation the burning rate. Also, the Zeldovich mechanism and Arrhenius equation form for engine knock prediction were considered in the modeling. The results showed that the lowest fuel consumption was obtained at high power and low emissions. It was noted that the compression ratio relevant to the lowest fuel consumption varies with speed of the engine. As an example, at engine speed of 1500 rpm, the lowest fuel consumption of about 200 gr/(kW-hr) was obtained at inlet conditions of 200 kPa and 333 K and compression ratio of 12.

Al-Baghdadi [35] has presented cycle computer simulation including the two-zone model to predict four stoke SI engine performance and emissions fuelled by gasoline, ethanol, hydrogen and their mixture. Calculation of burning rate and combustion duration was done using laminar and tubular theory of flame speed. Also, pre-ignition and knock occurrence were taken into account. The model compared performance parameters such as power, SFC and carbon dioxide and nitric oxide emissions of the engine for different fuels. The measurements were done on hydrogen-ethanol-gasoline fueled engine at stoichiometric mixture, MBT at 1500 rpm and compression ratio of 7.5. A very close agreement with experimental measurements was observed for this modeling. The results showed that the engine power increased by increasing the percentage of hydrogen up to 2% by mass due to increased mass burning rate. For more than 2% mass fraction of hydrogen, the power decreased as volumetric efficiency is reduced. Also, engine power increased with the increase in ethanol percentage up to 30% by volume. The author reported that the carburetor was not capable of evaporating all the supplied fuel for more than 30% volume fraction of ethanol and as a result the power and thermal efficiency was reduced. It was seen that CO emission decreased with increase of the percentage of hydrogen and/or ethanol. In contrast, NO_x concentrations increased when increasing the percentage of hydrogen or ethanol. The effects of compression ratio, equivalence ratio and engine speed on the performance and emission characteristics of a hydrogen fuelled SI engine has been investigated by the author in the another work [36].

Combustion in the SI engine is an extremely complex phenomenon and some models have been developed with different levels of capability to simulate the physical and chemical processes. In the simplest approach, the zero-dimensional model is used to predict combustion process in the cylinder. Whereas combustion occurs at constant volume instantaneously, the cylinder is presented by only one zone. Alla [28] declared that this assumption would increase IMEP and the power of the engine by some 50% relative to the real values. In quasi-dimensional model the entire cylinder contains two zones: burned and unburned. The combustion occurs during a progressive process. Obviously, this model is more accurate than the zero-dimensional model. In the three-zone model, the entire combustion chamber is divided into unburned zone, adiabatic burned zone, and a boundary layer burned zone [30]. Beside, multidimensional computational fluid dynamics (CFD) simulations are used for comprehensive study of the combustion process. This approach considers the chemical reactions mechanism which contains too many species, and so, it needs considerable usage of computer memory. This approach permits a better presentation of in-cylinder temperature and nitric oxide emission in comparison to other mentioned models [30]. In the present work, objective of the model is based on thermodynamic simulation to predict performance characteristics of the engine and parametric studies. Therefore the two-zone model for the combustion process simulation has been applied according to requirements. This selection and conformity has been confirmed by Heywood [37].

Research was carried out by D'Errico [22] on prediction of the combustion process and emissions of bi-fuelled gasoline and CNG SI engine by thermodynamic quasi-dimensional modeling and was validated by available experimental data. He presented a new correlation for laminar flame speed of methane–air mixtures by interpolating many different conditions at high pressure and temperature including consideration of a detailed chemical approach. The use of the new correlation to describe the combustion process was successful as good agreement was seen between relevant experimental and predicted in-cylinder pressure diagrams. Also, a reduced chemical scheme has been proposed by the author for species which are kinetically controlled. This mechanism showed a reliable prediction of in-cylinder carbon dioxide and nitric oxides emission. He reported that the good agreement between NO_x emissions as well as in-cylinder temperature profile predicted by quasi-dimensional modeling with CFD analysis showed the validity of the simplifications made in the quasi-dimensional simulation.

Thurnheer et al. [38] carried out a heat release and loss analysis of a naturally aspirated bi-fuel SI engine fuelled by gasoline, methane and blends containing methane and 5%, 10% and 15%vol hydrogen to investigate combustion differences between the fuels. The experiments were carried out at 2000 rpm, 2 bar BMEP and stoichiometric air fuel ratio to determine the spark timing for best fuel conversion efficiency. They measured the heat losses from the engine, the combustion duration and flame development angle as a function of spark timing. The main results of this paper indicated a decrease in the overall burn duration when the hydrogen fraction of the blend was increased. This was attributed to shorter time for the first stage of combustion.

The present work is an investigation on the performance characteristics and emissions of a bi-fuel spark ignition engine fuelled by gasoline and CNG using thermodynamic simulation of the engine closed cycle which has been reported by the authors primarily [39]. The simulation model has been based on the first law of thermodynamic in the non-differential equation form. The simplicity and ease of the solution of this approach is remarkable in prediction of temperature and pressure variations of the cylinder content resulting in engine perform-

ance and emissions. Stepwise calculations for in-cylinder pressure and temperature at compression process, ignition delay period, combustion and expansion processes have been considered. The performance characteristics including power, ISFC and specific emissions concentration of SI engine on both gasoline and CNG fuel are determined by the model. Measured data for the calibration and validation of the model has been used from available experimental tests that have been done on a bi-fuel SI engine. The effects of equivalence ratio, compression ratio and spark timing on power, ISFC and combustion duration have been investigated to show the capability of the model to predict engine performance characteristics.

2. Engine simulation model

2.1 Approach

The model has been used thermodynamically to simulate the closed power cycle of an SI engine including compression, ignition delay, combustion and expansion processes. Modeling is based on the first law of thermodynamics in its simple form and not in the differential form, therefore, the method is very simple and is easily understood while giving accurate results. Equations can not be solved analytically and the Newton-Raphson method has been used as a numerical solution technique [26]. Cylinder contents were treated as ideal gases and the equation of state were employed. During the compression, composition of the cylinder gas is considered constant, but, in the expansion stroke, the composition is changed in every interval due to dissociation reactions. The quasi-dimensional model has been used for simulation of the combustion process. The cylinder is divided into two zones which are separated by a thin flame front. The flame front is assumed to propagate spherically throughout the combustion chamber and each zone is spatially uniform. The heat transfer from cylinder content to the wall has been predicted with semi-empirical correlation proposed by Annand [37]. Heat transfer between burned and unburned zones and flow of gases into and out of the crevices of the cylinder were ignored in the simulation. The indicated work was approximated by integration of P-V diagram over each interval. The calculation procedure started with determination the temperature and the pressure in the compression stroke for every crank angle until the spark timing. After spark ignition, the ignition delay time was calculated and the flame front combustion was assumed to propagate spherically. After the combustion of the fuel, the entire volume of the cylinder was considered as a single zone filled with the combustion products for the expansion stroke. In the model developed, each stroke was divided into a number of intervals of small volume change. The time of each interval was determined by:

$$\Delta t = \frac{\Delta\theta}{360 \times n} \tag{1}$$

where Δθ (Deg.), n(rps) and Δt(s) denote crank angle change, engine speed and time interval, respectively. In every interval, the variation of the temperature and pressure were determined. The balancing the internal energy before and after each interval was checked using the first law of thermodynamics. If required, the estimated value of temperature was modified by the Newton-Raphson modification method. The calculation was repeated until the first law of thermodynamics was satisfied with the stipulated accuracy. The first estimate of temperature for the end of each interval was obtained by assuming an isentropic change for compression and expansion strokes.

2.2 Combustion model

In this study, a thermodynamic model, also known as the quasi-dimensional model has been used for combustion process simulation. The cylinder is divided into two zones, burned zone and unburned zone, separated by a thin flame front. The flame front propagates spherically throughout the combustion chamber until it reaches the cylinder walls. Each zone is assumed to be spatially homogeneous and the spark plug is located at the center of cylinder head. During combustion stroke, pressure is uniform throughout the cylinder, but there are two different temperature and composition for each zone. The composition of unburned gases is frozen while the composition of burned gases is in chemical equilibrium except for the nitrogen monoxide. Heat transfer between burned and unburned zones is ignored, but heat transfer from each zone to its surrounding surfaces is considered according Annand formula.

During the combustion process, the modeling of flame propagation in each crank angle is divided into four sub steps including: (1) compression of burned and unburned zones with inclusion of heat and work transfer, (2) combustion of a thin layer of the unburned zone and formation of a new burned zone, (3) temperature unification of new burned zone and old burned zone and (4) pressure equalization in the whole of cylinder. For every sub step and the values of temperature, pressure and burned gas composition are determined and they are modified by considering the conservation of energy. The combustion process was assumed to be finished when up to 99.99% by mass fraction of fuel is consumed. The overall equation for combustion of the fuel is considered as:

$$\begin{aligned} &C_nH_mO_x + (n + \frac{m}{4} - \frac{x}{2})\frac{1}{\phi}(O_2 + 3.7619N_2) \rightarrow \\ &a_1CO_2 + a_2CO + a_3H_2O + a_4H_2 + a_5N_2 + a_6O_2 \\ &+ a_7C_nH_mO_x + a_8NO + a_9O + a_{10}H + a_{11}OH + a_{12}N \end{aligned} \tag{2}$$

where $C_nH_mO_x$ indicates the definition of fuel formula. In this study, the effect of fuel composition has been considered according to different values of n, m, and x for each fuel. Values of n, m, and x are 7.13, 13.74 and 0.05 for gasoline and 1.13, 4.22 and 0.02 for CNG. It is obvious that there would be different composition of products due to variation of stoichiometic coefficients a_1 to a_{12} for each fuel considered.

2.2.1 Ignition delay calculation

The duration between spark timing and flame appearance in the cylinder is called the ignition delay time and is expresses as crank angle. According to Benson et al. [26] the flame appears in cylinder once the volume of the burned zone is equal to 0.001 of the total cylinder volume. The volume of the flame will be calculated by considering spherical propagation of the flame front. The flame speed indicates flame front propagation speed, and the flame radius variation can be calculated by:

$$\Delta r_f = \frac{S_T \times \Delta\theta}{360 \times n} \tag{3}$$

where r_f(m), S_T(m/s), θ (Deg.) and n(rps) are the flame radius, tubular flame speed, crank angle and engine speed, respectively.

2.2.2 Flame speed calculation

In this model, dependency of laminar flame speed on temperature and pressure of cylinder content is described by the empirical expression of Kuehl [40]:

$$S_L = \left[\frac{7780.8}{\left(\frac{10000}{T_b} + \frac{900}{T_u} \right)^{4.938}} \right] P^X \tag{4}$$

where P(bar), T_u(K), T_b(K) and S_L(m/s) are cylinder pressure, unburned zone temperature, burned zone temperature and laminar flame speed, respectively. In this experimental based model, X is a fitting parameter based on compatibility of simulated pressure-time diagram with the corresponding experimental data. This parameter is proposed to be equal to -0.09876 for propane-air mixture. Benson et al. [26] have used this equation for spark ignition engines and found good agreement between theoretical and experimental findings. Mozafari [41] has used this equation for fuels such as gasoline, propane, methanol and ammonia for prediction of spark ignition engine characteristics and found reasonable agreement with corresponding experimental data. In the present study, the same approach was applied and the proper values of X have been determined for gasoline and CNG fuels.

The relationship between the turbulent flame speed and laminar flame speed is modeled as [26]:

$$\frac{S_T}{S_L} = ff \tag{5}$$

where *ff*, S_L(m/s) and S_T(m/s) are flame factor, laminar flame speed and tubular flame speed, respectively.

According to Hiroyasu and Kadota [42] the flame factor correlates with the engine speed as:

$$ff = 1 + b \times N\,(rpm) \tag{6}$$

where b is a constant between 0.0017 and 0.0020 and is related to the type of engine and turbulence. The calibration of the flame factor is done by comparing a simulated cylinder pressure trace to a measured one, and matching the location of peak pressure in the two diagrams. Once the model has been calibrated for operation conditions including engine speed and equivalence ratio at the corresponding experiment, the calibration coefficients are assumed constant. For other input conditions the parameters must be calibrated again.

2.2.3 Calculation of burned zone area and volume

With the progress of the combustion process in the cylinder, the volume of unburned zone is reduced and that of the burned zone is increased. The flame front propagates throughout the combustion chamber. The volume of burned zone is calculated by considering spherical geometry of flame as it contacts with combustion walls. The calculation is based on the method developed by Chin et al. [43]. In order to consider the effect of turbulence on the flame speed propagation they have studied fractal geometry of the flame and developed Eq. (7) to (11) for burned zone volume, V_f(m^3)

$$V_f = \left(\frac{\pi}{8}\right) B^3 \left\{ \left(\frac{1}{3} \left(\frac{2r_f}{B} \right)^3 \left[\alpha^3 - \beta^3 - 3(\alpha - \beta) \right] \right) + \frac{2r_f \alpha}{B} \right\} \tag{7}$$

where B(m) and r_F(m) cylinder bore and flame radius, respectively. α and β are calculated as follows:

$$\alpha = 0 \qquad if \quad r_f < \frac{B}{2} \tag{8}$$

$$\alpha = \sqrt{1 - \left(\frac{B/2}{r_f} \right)^2} \qquad if \quad r_f > \frac{B}{2} \tag{9}$$

$$\beta = 1 \qquad if \quad r_f < h_{gap} \tag{10}$$

$$\beta = \frac{h_{gap}}{r_f} \qquad if \quad r_f > h_{gap} \tag{11}$$

where h_{gap}(m) indicates the instantaneous height of combustion chamber.

Also, a good estimation for area of burned zone A_f(m^2) is obtained as follows [43]:

$$A_f = \frac{\pi}{4} B^2 \left(2 \left[\frac{2r_f}{B} \right]^2 [\beta - \alpha] \right). \tag{12}$$

2.2.4 Engine knock modeling

Abnormal combustion causes serious damages to the engine due to sudden increase of temperature and pressure in end gas region of the flame front. This phenomena, knock, releases high chemical energy that is accompanied with pressure wave and noise [44]. For the prediction of abnormal combustion and knock occurrence in the end gas region of the flame front, the following integral during combustion process from combus-

tion start time (t = 0) to the corresponding time (t) has been checked [37]:

$$\int_{t=0}^{t} \frac{dt}{\tau} \neq 1 \tag{13}$$

where τ (s) is induction time which is calculated by the model presented by Douaud and Eyzat [44] as follows:

$$\tau = 17.68\left(\frac{ON}{100}\right)^{3.4107} p^{-1.7} \exp\left(\frac{3800}{T}\right) \tag{14}$$

where τ (ms), ON, p(atm) and T(K) are induction time, octane number of the fuel, in-cylinder pressure and mean temperature of burned and unburned zones, respectively. In the present model, Eq. (13) is evaluated and if the equation is not satisfied, the calculation procedure is terminated.

2.2.5 Rate kinetics

According to the overall equation for combustion of the fuel (Eq. (2)), twelve species, namely CO_2, CO, H_2O, H_2, N_2, O_2, UHC, O, H, OH, N and NO have been considered. It can be assumed that except NO, all other species are in thermodynamic equilibrium due to fast reaction rates as in the following:

$$CO + \frac{1}{2}O_2 \leftrightarrow CO_2 \tag{15}$$

$$CO + H_2O \leftrightarrow CO_2 + H_2 \tag{16}$$

$$nCO_2 + {}^{m}\!/_{2}\, H_2 \leftrightarrow C_nH_mO_x + (n - {}^{x}\!/_{2})O_2 \tag{17}$$

$$H_2O + {}^{1}\!/_{2}\, N_2 \leftrightarrow H_2 + NO \tag{18}$$

$$O_2 \leftrightarrow 2O \tag{19}$$

$$H_2 \leftrightarrow 2H \tag{20}$$

$$H_2O \leftrightarrow OH + {}^{1}\!/_{2}\, H_2 \tag{21}$$

$$N_2 \leftrightarrow 2N. \tag{22}$$

Therefore, eight non-linear equations based on the equilibrium constant expressions for reactions (15)-(22) with four linear equations obtained from the conservation of the atomic mass of O, H, N and C can be written. Numerical solution of these equations at an assumed corresponding combustion temperature determines the equilibrium mole number of each product. Then the accuracy of the first law of thermodynamics is checked according to the calculated composition and the corresponding temperature. If the balance of internal energy of the reactants and products is not achieved in the range of the stipulated accuracy, the combustion temperature is modified by Newton-Raphson method until a solution is achieved.

The formation of NO is rate limited due to very high dependency on temperature. Therefore, the extended Zeldovich mechanism has been used as the basic model for non-equilibrium NO formation:

$$O + N_2 \xleftrightarrow{1} NO + N \tag{23}$$

$$N + O_2 \xleftrightarrow{2} NO + O \tag{24}$$

$$N + OH \xleftrightarrow{3} NO + H. \tag{25}$$

The rate constants of each reaction can be determined as [45]:

$$k_{1b} = 3.8\times10^{13} \exp(-425/T) \tag{26}$$

$$k_{1f} = 1.8\times10^{14} \exp(-38370/T) \tag{27}$$

$$k_{2b} = 3.8\times10^{9}\, T \exp(-20820/T) \tag{28}$$

$$k_{2f} = 1.8\times10^{10}\, T \exp(-4680/T) \tag{29}$$

$$k_{3b} = 1.7\times10^{14} \exp(-24560/T) \tag{30}$$

$$k_{3f} = 7.1\times10^{13} \exp(-450/T) \tag{31}$$

where $k\,(cm^3.mol^{-1}.s^{-1})$ and T(K) are rate constants and temperature, respectively. By considering Eq. (23) to (25), the net rate of NO formation is calculated by:

$$\frac{d[NO]}{dt} = k_{1f}[O][N_2] - k_{1b}[NO][N] + k_{2f}[N][O_2] - k_{2b}[NO][O] + k_{3f}[N][OH] - k_{3b}[NO][H] \tag{32}$$

where [] denotes the concentration of the species per cubic centimeter. To derive an expression for the rate of NO formation, the following equations can be used for the equilibrium reactions (23) to (25):

$$R_1 = k_{1f}[O]_e[N_2]_e = k_{1b}[NO][N]_e \tag{33}$$

$$R_2 = k_{2f}[N]_e[O_2]_e = k_{2b}[NO][O]_e \tag{34}$$

$$R_1 = k_{1f}[N]_e[OH]_e = k_{1b}[NO][H]_e. \tag{35}$$

As mentioned, the O, H and OH radicals remain in thermodynamic equilibrium while the rate of N formation can be assumed at steady state. Therefore, the net rate of NO formation is obtained by regarding $[O] = [O]_e$, $[H] = [H]_e$, $[OH] = [OH]_e$ and $[N] = [N]_e$ and substituting Eqs. (33)-(35) in the Eq. (32):

$$\frac{d[NO]}{dt} = \frac{2R_1\left(1 - \left(\frac{[NO]}{[NO]_e}\right)^2\right)}{1 + \frac{[NO]}{[NO]_e}\left(\frac{R_1}{R_2 + R_3}\right)}. \tag{36}$$

At first, the model calculates the equilibrium concentration of the NO($[NO]_e$) by considering reactions (15) to (22). Then this value is considered for the determination of non-equilibrium concentration of NO in Eq. (36) which has been

Table 1. Engine specifications.

Engine type	XU7 JP/L3
Number of cylinder	4
Bore (mm)	83
Stroke (mm)	81.4
Con. rod length (mm)	143.1
Load (%)	100
Equivalence ratio	1.1
Speed (rpm)	1500-4000
Spark timing (bTDC)	MBT
Compression ratio	9.2
IVO [deg] @ 1 mm lift	8.5 TDC
IVC [deg] @ 1 mm lift	29.3 aBDC
EVO [deg] @ 1 mm lift	43.3 bBDC
EVC [deg] @ 1 mm lift	5.5 aTDC

Table 2. Natural gas composition (% vol.).

C_1	C_2	C_3	C_4	C_5
90.6	4.5	1.1	0.4	0.11
C_6	CO_2	N_2	O_2	S_2
0.08	0.93	2.28	0	0

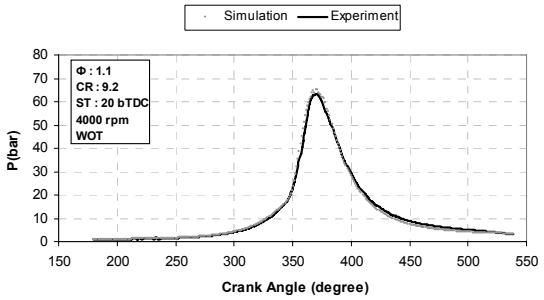

Fig. 1. Cylinder pressure versus crank angle for gasoline fuelled engine (●Simulation, — Experiment).

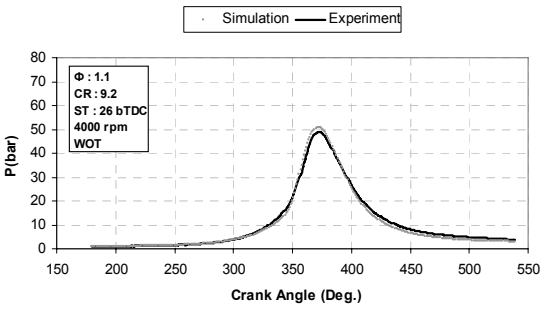

Fig. 2. Cylinder pressure versus crank angle for CNG fuelled engine (●Simulation, — Experiment).

solved numerically by the Runge-Kutta forth order method. According to Mustafi et al. [46], as the temperature falls below 2000-2300 K the NO reaction rate becomes very slow and the NO concentration effectively freezes at a value greater than the equilibrium value. In this simulation, in order to calculation the frozen value of NO, the temperature has been assumed to be 2000 K.

3. Results and discussion

3.1 Model validation

The results of thermodynamic modeling have been compared with available experimental data including indicated power, ISFC and specific emissions. Experimental tests were carried out in the engine test laboratory of Irankhodro Powertrain Company (IPCO) and used by the authors to validate of the model. The tests were carried out on a XU7 JP/L3 four cylinder research SI bi-fuel engine, which was fuelled by gasoline and CNG with various ranges of speed, WOT condition, MBT spark timing and at a compression ratio of 9.2. Engine specifications are shown in Table 1. Gasoline composition with LHV of 43.12 MJ/kg was carbon 85.55, hydrogen 13.74 and oxygen 0.71 mass fraction percentages and, the composition of natural gas with LHV of 46.75 MJ/kg is shown in Table 2.

3.1.1 Pressure of the cylinder

Figs. 1 and 2 show the variations of cylinder pressure with respect to crank angle at 4000 rpm for gasoline and CNG fuelled engine, respectively. According to these figures, the predicted pressure change shows good agreement with the pressure trace taken from the experimental tests. Comparison of in-cylinder pressure data for both experiments and the model shows an idea of the burning rate model's validity for these fuels.

To find the proper flame factor in Eq. (6) and therefore the turbulent flame speed, the predicted pressure-crank angle diagram has been compared to the experimental pressure data. The peak pressures in the simulated and experimental diagrams are matched together and flame factor (ff in Eq. (6)) is determined to be 6.2 at 4000 rpm and equivalence ratio of 1.1 for gasoline. For CNG the value obtained is 7.8 at similar conditions. The corresponding flame factors were set as the base for calculations at 4000 rpm and the proper flame factor must be calibrated for other engine speed. It is expected that flame factor of CNG should be more than that of gasoline due to more spark advance. Also, the pressure peak of gasoline fuelled engine is higher than that of CNG due to higher volumetric efficiency.

3.1.2 Indicated power and indicated specific fuel consumption

Fig. 3 shows the engine indicated power in the range of 1500 – 4000 rpm engine speed for gasoline and CNG fuelled engine. The computed power is the time variation average of the net work transferred from gas cylinder to the piston during compression to expansion strokes. This figure shows reasonable agreement between the model results and the experimental data for both fuels. Higher indicated power at higher en-

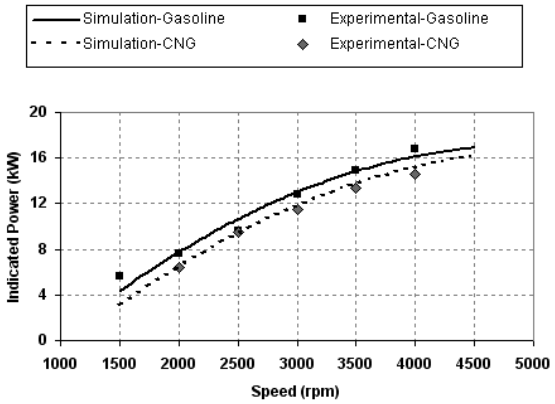

Fig. 3. Indicated power versus engine speed for gasoline and CNG fuelled engine, (Ø: 1.1, CR: 9.2, ST: 20 (gasoline), 26 (CNG), WOT).

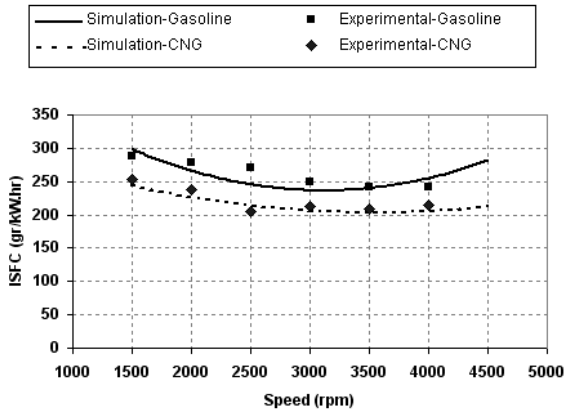

Fig. 4. ISFC versus engine speed for gasoline and CNG fuelled engine,(Ø: 1.1, CR: 9.2, ST: 20 (gasoline), 26 (CNG), WOT).

gine speeds are due to increases in the number of cycles per unit time. Also, power of the gasoline-fuelled engine is higher than that of the CNG fuelled one, which is due to higher volumetric efficiency of this fuel. In fact, smaller volume of the cylinder is occupied by air at the intake stroke when using CNG and it could be concluded that the CNG fuelled engine has lower volumetric efficiency. According to the Fig. 3, the power of CNG fuelled engine is reduced roughly by 11% over the speed range of 1500 to 4000 rpm.

Predictions of the fuel consumption based on this model were found to conform quite well with the corresponding reported measured data. The effect of engine speed on ISFC is shown in Fig. 4. It was found that the engine fuel consumption decreased by about 15% from 298 to 252 gr/(kW-hr) for gasoline and from 240 to 204 gr/(kW-hr) for CNG over the speed range of 1500 to 4000 rpm. This is due to increase of indicated thermal efficiency when increasing the engine speed. In average, the data shows about 16% reduction of ISFC when the engine was operated using CNG. Because the LHV of CNG is higher than that of gasoline, the fuel consumption of the engine is decreased when fuelled with CNG.

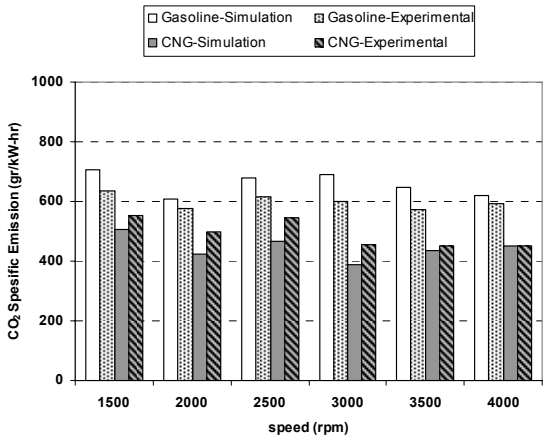

Fig. 5. Comparison of CO_2 specific emission for gasoline and CNG fuelled engine with experimental data, (Ø: 1.1, CR: 9.2, ST: 20 (gasoline), 26 (CNG), WOT).

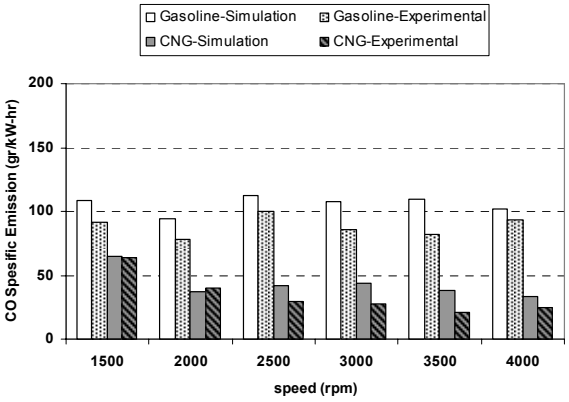

Fig. 6. Comparison of CO specific emission for gasoline and CNG fuelled engine with experimental data, (Ø: 1.1, CR: 9.2, ST: 20 (gasoline), 26 (CNG), WOT).

3.1.3 Emissions

Figs. 5-8 illustrate the effect of fuel type on engine exhaust gases. According to these findings, the predicted specific emissions are in good agreement with the corresponding experimental results for CO_2, CO, UHC and NO species.

It can be seen from Fig. 5 that the specific emission of CO_2 in CNG fuelled engine is lower than when using gasoline. This is because the main component of CNG is methane with a lower carbon to hydrogen ratio than gasoline. The same trend is seen for CO concentration as shown in Fig. 6. This is due to lower carbon to hydrogen ratio of CNG and more efficient combustion as a result.

Figs. 7 and 8 present the concentration of UHC and NO species when the engine is operated with each of the fuels. The UHC sources in an SI engine are flame quenching, crevices, valve leakage, oil layers, deposits, liquid fuel, and more importantly incomplete combustion [3]. In this study the only source considered was incomplete combustion. As for gasoline, the share of UHC from incomplete combustion is much bigger than the other phenomena, the trends for UHC concen-

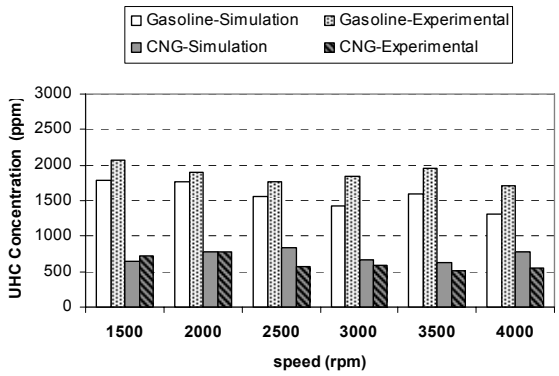

Fig. 7. Comparison of UHC concentration for gasoline and CNG fuelled engine with experimental data, (Ø: 1.1, CR: 9.2, ST: 20 (gasoline), 26 (CNG), WOT).

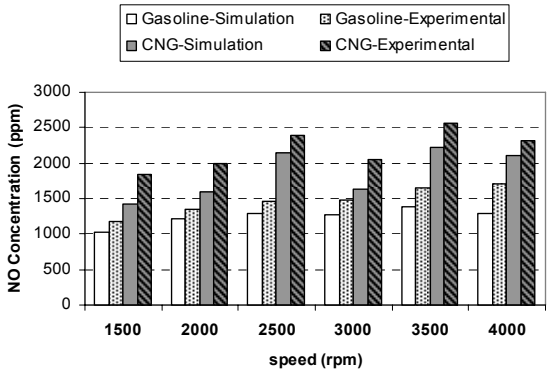

Fig. 8. Comparison of NO concentration for gasoline and CNG fuelled engine with experimental data, (Ø: 1.1, CR: 9.2, ST: 20 (gasoline), 26 (CNG), WOT).

tration with engine speed is predicted more accurately.

The results show some decrease in UHC concentration when using CNG. Higher combustion temperature of CNG fuelled engine results in better combustion of the fuel. As expected, the NO concentration is increased when using CNG due to strong dependence of NO concentration on temperature. There are two reasons for higher combustion temperature in CNG fuelled engine. Firstly, LHV of CNG is higher than that of gasoline; and secondly, carbon to hydrogen ratio of CNG is also lower. It should be noted that spark retarding, leaner burning method and EGR are three methods for the reduction of NO concentration in CNG engine.

According to Figs. 5 to 8, for speed range of 1500-4000 rpm, the specific emissions of CO_2, CO and concentration of UHC are decreased considerably by about 33%, 60% and 53%, respectively, but concentration of NO increased by 50% when CNG is used. These values are in the ranges that have been reported in Refs. [12, 13].

3.2 Parametric study

According to the previous section, the results obtained from the model show good agreement with experimental data.

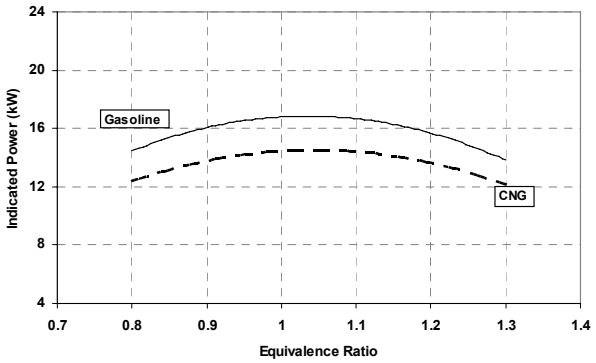

Fig. 9. Indicated power versus equivalence ratio for gasoline and CNG, (4000 rpm, CR: 9.2, ST: 20 (gasoline), 26 (CNG), WOT).

Therefore, simulation model has been used to evaluate the effects of equivalence ratio, compression ratio and spark timing on the engine performance characteristics. The reasonable results show the model is well constructed to describe the performance characteristics of the engine over a wide range of operating variables.

3.2.1 Effect of equivalence ratio

Equivalence ratio is an operational variable which affects the performance characteristics of the engine. Fig. 9 illustrates the variation of the engine indicated power for equivalence ratios in the range of 0.8 to 1.3 for gasoline and CNG operations. It can be seen that for both fuels, the maximum indicated power is obtained at equivalence ratio of about 1 to 1.1 due to more efficient combustion. Also as mention in Fig. 3, the indicated power of gasoline-fuelled engine is higher than that of CNG operation due to higher volumetric efficiency.

The effect of equivalence ratio on ISFC is presented in Fig. 10. Obviously, higher fuel consumption is obtained with increasing equivalence ratio due to richer cylinder mixture. Also, it is expected that fuel consumption of CNG fuelled engine is lower due to better combustion of CNG, having lower carbon to hydrogen ratio.

As expected, the combustion is most efficient for equivalence ratio of 1 to 1.1 and therefore the duration of combustion to release the fuel energy is minimum. As a result, it can be seen from Fig. 11 that the predicted combustion duration is lowest when the equivalence ration is near to 1 to 1.1. In this figure, the flame factor in the Eq. (6) has been calibrated for engine speed of 4000 rpm and equivalence ratio of 1.1 and is considered constant for all other equivalence ratios for this engine speed. Combustion duration is a function of flame factor and this assumption may lead to some error in the combustion duration predictions. However since the aim of this parametric study has been to compare two type of fuels, this error has not been considered and is assumed to have little effect on the results.

3.2.2 Effect of compression ratio

The indicated power is plotted with respect to the compres-

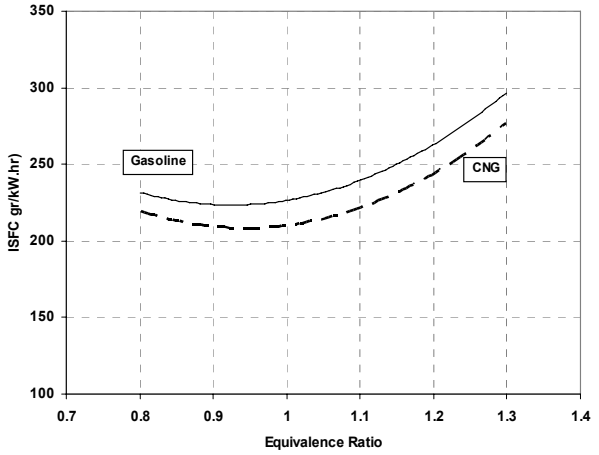

Fig. 10. ISFC versus equivalence ratio for gasoline and CNG, (4000 rpm, CR: 9.2, ST: 20 (gasoline), 26 (CNG), and WOT).

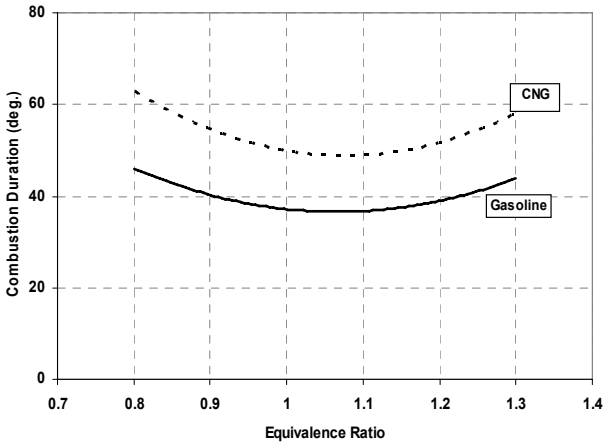

Fig. 11. Combustion duration versus equivalence ratio for gasoline and CNG, (4000 rpm, CR: 9.2, ST: 20 (gasoline), 26 (CNG), WOT).

sion ratio in Fig. 12. The indicated power of both fuels is increased when the increasing the compression ratio due to higher pressure at the start of combustion process. As expected, at the same condition, the power of gasoline fuel is more than that of CNG fuel. The engine power rises roughly by 19% over the compression ratio range of 7 to 11.

The effect of compression ratio on ISFC has been shown in Fig. 13. The ISFC decreases by about 15% in gasoline operation and 20% in CNG operation for compression ratio ranging from 7 to 11. Also, the combustion duration is reduced in this range. This is due to the fact when the pressure of the cylinder content is increased, the combustion process occurs more efficiently and therefore ISFC and ignition delay decrease (Fig. 14).

3.2.3 Effect of spark timing

In the SI engine, if ignition occurs too early, work will be wasted in the compression stroke. On the other hand, if ignition is too late, the indicated power is lower due to lower peak pressure of the combustion. Therefore, there is an optimum

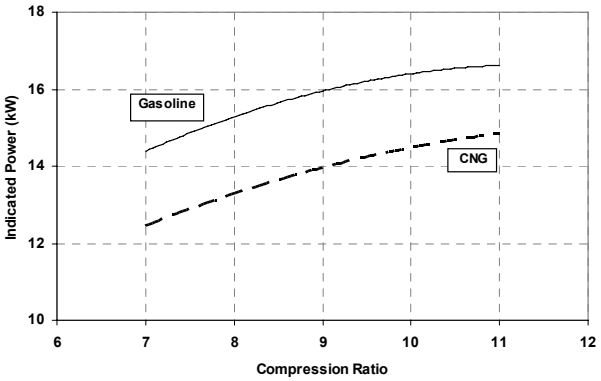

Fig. 12. Indicated power versus compression ratio for gasoline and CNG, (Ø: 1.1, 4000 rpm, ST: 20 (gasoline), 26 (CNG), WOT).

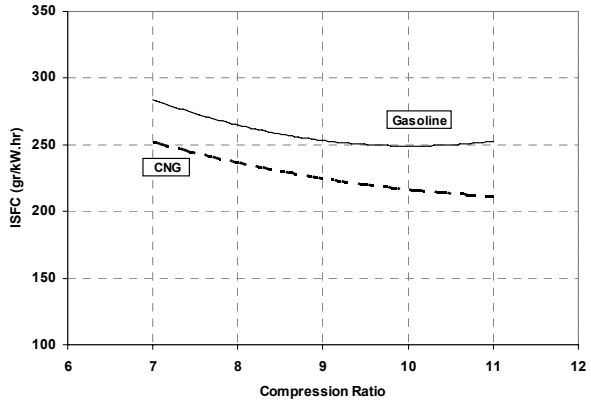

Fig. 13. ISFC versus compression ratio for gasoline and CNG, (Ø: 1.1, 4000 rpm, ST: 20 (gasoline), 26 (CNG), WOT).

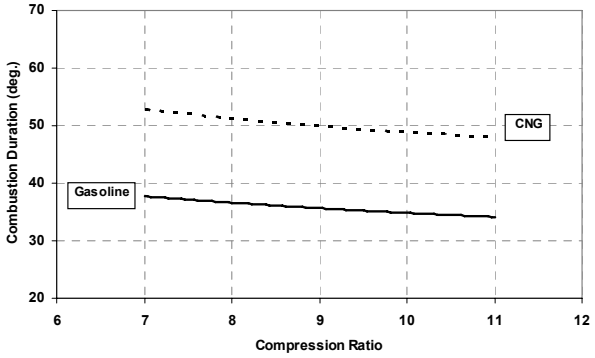

Fig. 14. Combustion duration versus compression ratio for gasoline and CNG, (Ø: 1.1, 4000 rpm, ST: 20 (gasoline), 26 (CNG), WOT).

spark timing at which the maximum torque is obtained. This timing is called MBT. It is clear that the indicated power is maximum at 20 bTDC for gasoline and 26 bTDC for CNG operations. These trends were shown in Fig. 15.

In Fig. 16, the variations of ISFC with respect to spark timing are shown. According to this figure, the ISFC is minimum at MBT, where the power is maximum. As expected, for spark timing sooner or later than MBT, the fuel consumption is increased due to power decrease. These trends are also seen for

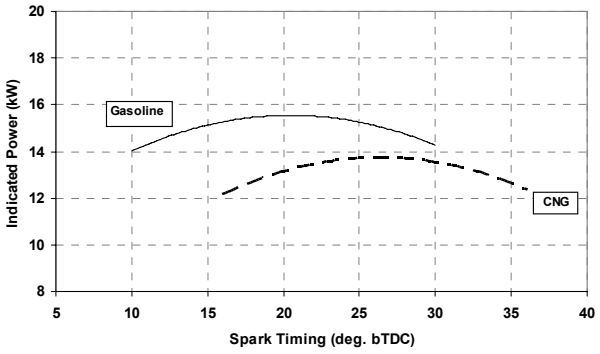

Fig. 15. Indicated power versus spark timing for gasoline and CNG, (Ø: 1.1, CR: 9.2, 4000 rpm, WOT).

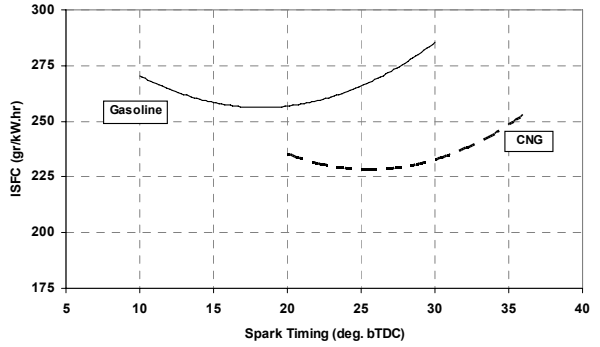

Fig. 16. ISFC versus spark timing for gasoline and CNG, (Ø: 1.1, CR: 9.2, 4000 rpm, WOT).

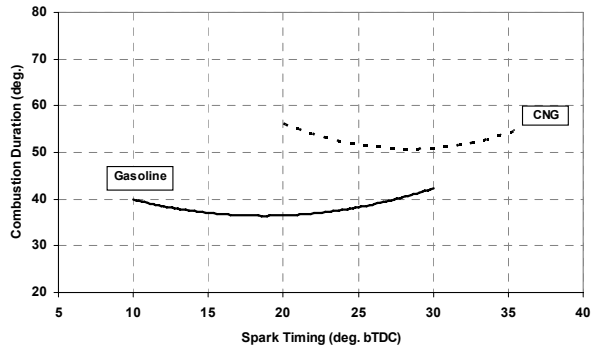

Fig. 17. Combustion duration versus spark timing for gasoline and CNG, (Ø: 1.1, CR: 9.2, 4000 rpm, WOT).

the combustion duration in Fig. 17 and the shortest combustion duration belongs to MBT advance spark timing.

4. Conclusions

In this study, a thermodynamic cycle simulation model for a conventional four-stroke spark ignition engine has been developed. The model is primarily based on the first law of thermodynamics. The simulated power cycle was a closed cycle which included compression, ignition delay, combustion and expansion processes. The stepwise calculations for pressure and temperature of the cylinder at compression process, ignition delay time, combustion and expansion processes have been considered. Two-zone model for the combustion process simulation has been used. The performance characteristics and emissions concentration of SI engine were predicted by the model for gasoline and CNG operations. The predicted pressure change has good agreement with the pressure trace taken from the experimental reported results. Also, the predicted results for engine performance characteristics and emission formations showed reasonable agreement with the corresponding experimental data for a range of engine speed. These conformities have validated the developed thermodynamic model. The results have shown that the power of CNG fuelled engine is lower than that of gasoline fuelled engine by about 11% over the speed range of 1500 to 4000 rpm due to higher volumetric efficiency. In average, when the engine operates with CNG fuel, the ISFC is reduced roughly 16% over this speed range. However for this engine speed range the specific emissions of CO_2, CO and concentration of UHC are decreased considerably by about 33%, 60% and 53%, respectively, while NO concentration increased by 50%. Finally, parametric studies have been carried out for investigation of the effect of equivalence ratio, compression ratio and spark timing on the indicated power, ISFC and combustion duration using the developed model to describe the performance characteristics of the engine over a range of operating variables.

Acknowledgements

The authors wish to thank from the laboratory of engine test of Irankhodro Powertrain Company (IPCO) and Mr. Ahmad Shafiei Sabet for providing the experimental data.

Nomenclature

Symbols

a : Stoichiometric coefficient
A : Area
B : Cylinder bore
h : Instantaneous height of combustion chamber
k : Rate constant
m : Number of atomic hydrogen in hydrocarbon fuel
N : Engine speed (rpm)
n : Engine speed (rps)
n : Number of atomic carbon in hydrocarbon fuel
p : Cylinder pressure
r : Radius
S : Flame speed
t : Time
T : Temperature
V : Volume,
x : Number of atomic oxygen in hydrocarbon fuel

Greek symbols

θ : Crank angle

ϕ : Equivalence ratio
τ : Induction time

Subscripts

b : Burned zone, backward
f : Flame, forward
gap : Cylinder gap
i : Species i
L : Laminar
T : Turbulent
u : Unburned

Notations

Δ : Difference
$\bar{}$: Average or mean value
[] : Concentration

Abbreviations

aBDC : After BDC
aTDC : After TDC
bBDC : Before BDC
bTDC : Before TDC
BMEP : Break mean effective pressure
BSFC : Break specific fuel consumption
CNG : Compressed natural gas
CR : Compression ratio
EVC : Exhaust valve closing
ff : Flame factor
EVO : Exhaust valve opening
ISFC : Indicated specific fuel consumption
IVC : Inlet valve closing
IVO : Inlet valve opening
LHV : Low heating value
MBT : Maximum brake torque
ON : Fuel octane number
ppm : Parts per million
SI : Spark ignition
ST : Spark timing
UHC : Unburned hydrocarbons
WOT : Wide open throttle

References

[1] J. Romm, The car and fuel of the future, *Energy Policy,* 34 (2006) 2609-2614.
[2] S. Yedla and R. M. Shrestha, Multi-criteria approach for the selection of alternative options for environmentally sustainable transport system in Delhi, *Transportation Research Part A,* 37 (2003) 717-729.
[3] R. R. Maly, State of the art and future needs in S.I. engine combustion, *25th Symposium (International) on Combustion* (1994) 111-124.
[4] A. M. K. P. Taylor, Science review of internal combustion engines, *Energy Policy,* 36 (2008) 4657-4667.
[5] S. Shiga, S. Ozone, H. T. C. Machacon, T. Karasawa, H. Nakamura, T. Ueda, N. Jingu, Z. Huang, M. Tsue and M. Kono, A study of the combustion and emission characteristics of compressed natural gas direct-injection stratified combustion using a rapid-compression-machine, *Combustion and Flame,* 129 (2002) 1-10.
[6] B. A. Abbanat, Alternative fuel vehicles: The case of compressed natural gas (CNG) vehicles in California households, *M.Sc. Thesis*, University of California, Davis, USA (2001).
[7] M. U. Aslam, H. H. Masjuki, M. A. Kalam, H. Abdesselam, T. M. I. Mahlia and M. A. Amalina, An experimental investigation of CNG as an alternative fuel for a retrofitted gasoline vehicle, *Fuel,* 85 (2006) 717-724.
[8] M. P. Hekkerta, F. H. J. F. Hendriksa, A. P. C. Faaijb and L. N. Maarte, Natural gas as an alternative to crude oil in automotive fuel chains well-to-wheel analysis and transition strategy development, *Energy Policy*, 33 (2005) 579-594.
[9] L. C. Olivier and P. Frédéric, Nox emissions reduction of a natural gas SI engine under lean conditions: comparison of the EGR and RGR concepts, *Proc. of ICES06 Spring Technical Conference of the ASME Internal Combustion Engine*, Aachen, Germany, (2006).
[10] H. M. Cho and B. He, Spark ignition natural gas – a review, *Energy Conversion and Management*, 48 (2007) 608-618.
[11] Z. Ristovski, L. Morawska, G. A. A. Yoko, G. Johnson, D. Gilbert and C. Greenaway, Emissions from a vehicle fitted to operate on either petrol or compressed natural gas, *Science of the Total Environment,* 323 (2004) 179-194.
[12] M. U. Aslam, H. H. Masjuki, M. A. Kalam, H. Abdesselam, T. M. I. Mahlia and M. A. Amalina, An experimental investigation of CNG as an alternative fuel for a retrofitted gasoline vehicle, *Fuel,* 85 (2006) 717-724.
[13] A. H. Shamekhi, N. Khatibzadeh and A. Shamekhi, A comprehensive comparative investigation of compressed natural gas as an alternative fuel in a bi-fuel spark ignition engine, *Iranian Journal of Chemistry and Chemical Engineering*, 27 (2008) 73-83.
[14] L. Guzzella, *Introduction to modeling and control of internal combustion engine systems*, Springer (2004).
[15] O. Badr, G. A. Karim and B. Liu, An examination of the flame spread limits in a dual fuel engine, *Applied Thermal Engineering* , 19 (1999) 1071-1080.
[16] K. M. Chun and J. B. Heywood, Estimating heat- release and mass-of-mixture burned from spark ignition engine pressure data, *Combustion Science and Technology*, 54 (1987) 133-143.
[17] R. Lanzafame and M. Messina, ICE gross heat release strongly influence by specific heat ratio values, *International Journal of Automotive Technology*, 4 (2003) 125-133.
[18] O. Yasar, A new ignition model for spark ignited engine simulations, *Parallel Computing*, 27 (2001) 179-200.
[19] F. Battin-Leclerc, P. A. Glaude, V. Warth, R. Fournet, G. Scacchi and G. M. Come, Computer tools for modeling the

chemical phenomena related to combustion, *Chemical Engineering Science,* 55 (2000) 2883-2893.

[20] R. Harish Kumar and A. J. Antony, Progressive combustion in SI engines- experimental investigation on influence of combustion related parameters, *Sadhana*, 33 (2008) 821-834.

[21] H. Batraktar and O. Durgun, Development of an empirical correlation for combustion durations in spark ignition engines, *Energy Conversion and Management*, 45 (2004) 1419-1431.

[22] G. D'Errico, Prediction of the combustion process and emission formation of a bi-fuel S.I. engine, *Energy Conversion and Management*, 49 (2008) 3116-3128.

[23] W. Pulkrabek, *Engineering fundamentals of the internal combustion engine*, Second Ed. Pearson Prentice-Hall, Upper Saddle River, New Jersey (2004).

[24] A. M. K. P. Taylor, Science review of internal combustion engines, *Energy Policy*, 36 (2008) 4657-4667.

[25] S. Verhelst and C. G. W. Sheppard, Multi-zone thermodynamic modeling of spark ignition engine combustion – an overview, *Energy conversion and Management*, 50 (2009) 1326-1335.

[26] R. S. Benson, W. J. D. Annand and P. C. Baruatt, A simulation model including intake and exhaust system for a single cylinder four-stroke cycle spark ignition engine, *International Journal of Mechanical Science*, 17 (1975) 97-124.

[27] C. D. Rakopoulos, Evaluation of a spark ignition engine cycle using first and second law analysis techniques, *Energy conversion and Management*, 34 (12) (1993) 1299-1314.

[28] A. G. H. Alla, Computer simulation of a four stroke spark ignition engine, *Energy conversion and Management*, 43 (2002) 1043-1061.

[29] L. Eriksson and I. Andersson, An analytic model for cylinder pressure in a four stroke SI engine, *SAE paper*, 2002-01-0371 (2002).

[30] J. A. Caton, A cycle simulation including the second law of thermodynamics for the spark-ignition engines: implications of the use of multiple-zones for combustion, *SAE paper*, 2002-01-007 (2002).

[31] J. A. Caton, Effects of the compression ratio on nitric oxide emissions for a spark ignition engine: results from a thermodynamic cycle simulation, *International Journal of Engine Research*, 4 (4) (2003) 249-268.

[32] Y. Ge, L. Chen, F. Sun and C. Wum, Thermodynamic simulation of performance of an Otto cycle with heat transfer and variable specific heats of working fluid, *International Journal of Thermal Science*, 44 (2005) 506-511.

[33] E. Abu-Nada, I. Al-Hinti, A. Al-Sarkhi and B. Akash, Thermodynamic modeling of spark-ignition engine: Effect of temperature dependent specific heats, *International Comunications in Heat and Mass Transfer*, 33 (2006) 1264-1272.

[34] A. Ibrahim and S. Bari, Optimization of a natural gas SI engine employing EGR strategy using a two-zone combustion model, *Fuel*, 87 (2007) 1824-1834.

[35] M. A. R. S. Al-Baghdadi, A simulation model for a single cylinder four-stroke spark ignition engine fueled with alternative fuels, *Turkish Journal of Engineering and Environmental Science*, 30 (2006) 331-350.

[36] M. A. R. S. Al-Baghdadi, Effect of compression ratio, equivalence ratio and engine speed on the performance and emission characteristics of a spark ignition engine using hydrogen as a fuel, *Renewable Energy*, 29 (2004) 2245-2260.

[37] J. B. Heywood, *Internal combustion engine fundamentals*, McGraw-Hill (1988).

[38] T. Thurnheer, P. Soltic and P. Dimopoulos Eggenschwiler, S.I. engine fuelled with gasoline, methane and methane/ hydrogen blends: heat release and loss analysis, *International Journal Hydrogen Energy,* 34 (2009) 2494-2503.

[39] M. Dashti, A. A. Hamidi and A. A. Mozafari, A comparative study of the performance of a SI engine fuelled by natural gas as alternative fuel by thermodynamic simulation, *Proc. of the ASME Internal Combustion Engine Fall Technical Conference (ICEF2009*), Lucerne, Switzerland (2009).

[40] J. B. Heywood, *Internal combustion engine fundamentals*, New York, Mc.Graw-Hill Inc., Chapters 4 and 9 (1988).

[41] D. K. Kuehl, Laminar burning velocity of propane-air mixture, *8th Symposium (International) on Combustion* (1962) 510.

[42] A. A. Mozafari, Prediction and measurement of spark ignition engine characteristics using ammonia and other fuels, *Ph. D. Thesis*, University of London (1988).

[43] H. Hiroyasu and T. Kadota, Computer simulation for combustion and exhaust emissions on spark ignition engine, *15th Symposium (International) on Combustion* (1974) 1213-1223.

[44] Y. Chin, R. D. Matthews, S. P. Nichols and T. M. Kiehne, Use of fractal geometry to model turbulent combustion in SI engines, *Combustion Science and Technology,* 86 (1992) 1-30.

[45] A. M. Douaud and P. Eyzat, Four-octane- number method for predicting the anti-knock behavior of fuels and engines, *SAE paper*, No.780080 (1978) 294-308.

[46] G. L. Borman and K. W. Ragland, *Combustion engineering*, McGraw Hill Inc., Chapter 4 (1998).

[47] N. N. Mustafi, Y. C. Miraglia, R. R. Raine, P. K. Bansal and S. T. Elder, Spark-ignition engine performance with power-gas fuel (mixture of CO/H2): A comparison with gasoline and natural gas, Fuel, 85 (2006) 1605-1612.

Mehrnoosh Dashti (Ph.D in Energy Engineering, Iran) worked at the energy saving sector of the National Iranian Industry Company (NIOC) as a research assistant between 2003 and 2005. She has served as lecturer at the department of Environment and Energy of SRBIAU and at the department of Mechanical Engineering of CTBIAU from 2005. She has done her Ph.D thesis on the thermodynamic simulation of internal combustion engines fuelled by CNG/gasoline blend. Her research interests are internal combustion engines, fuels and alternative energies and energy saving technologies, especially the modeling and simulation of ICE.